MEASURING ROAD STRUCTURES USING A MOBILE MAPPING SYSTEM

O. Grešla [1, 2], P. Jašek [1]

[1] Geodetická kancelář Nedoma & Řezník, s.r.o., 10200 Prague 10, Plukovnika Mraze 1425/1 – (gresla, jasek)@nedomareznik.cz
[2] Czech Technical University in Prague, Faculty of Civil Engineering, 16629 Prague 6, Thakurova 7 – ondrej.gresla@fsv.cvut.cz

KEY WORDS: Mobile Mapping Systém, Laser-scanning, Road Structures, Riegl, CloudCompare.

ABSTRACT:

The purpose of this thesis is to provide a detailed description of the Riegl VMX-2HA mobile mapping systém (MMS), its functions, composition and the data acquisition and processing procedure. In addition, this work presents a comparative analysis of the systém's height accuracy in relation to measurements made with the Leica NOVA MS50 multi-station. Using an experimental method, this study also shows that the order in which the described steps are performed can significantly affect the accuracy of the collected data. The results show that the use of the MMS in combination with appropriate data processing techniques can result in highly accurate data that can be used for a wide range of applications in the field of transportation infrastructure management and development. By providing a deeper understanding of the functions and capabilities of the MMS, this thesis describes valuable knowledge for professionals in the field seeking to optimize their data collection and analysis methods.

1. INTRODUCTION

The historical development of surveying methods has advanced from counting the rotations of a measuring vehicle's wheel, through GPSVan from the late 20th century (Coetsee et al., 1994) to today's modern methods of mobile mapping. However, certain principles have been borrowed from historical methods and improved with modern technologies, allowing us to achieve precision on the order of centimeters instead of meters. With a carefully chosen approach, we can attain even greater accuracy.

With the pressure to streamline the construction of transportation infrastructure, there is an emphasis on the rapid collection of comprehensive and spatially accurate data of road layers. Thanks to the mentioned advancements in surveying instrument development, we can utilize laser scanning on a moving vehicle - MMS - which provides us with a precise and more comprehensive view of road layers compared to commonly used methods.

Certainly, the applications of mobile scanners extend beyond the ones previously mentioned. In addition to their usage in collecting data for road layers, they are widely employed in the creation of digital technical maps. One notable advantage of mobile scanners is their ability to rapidly gather data, allowing for efficient mapping processes. Moreover, these scanners minimize the need for pedestrians to be actively involved in traffic, enhancing both safety and accuracy during data collection. By utilizing mobile scanners, surveyors can obtain detailed and precise information about the surrounding environment, including roads, buildings, and other infrastructure elements. This comprehensive data serves as a valuable resource for urban planning, infrastructure development, and maintenance, as well as various other applications requiring detailed spatial information. Therefore, mobile scanners play a crucial role in modern surveying practices, offering a faster and more efficient means of capturing data and creating digital maps. (Pavelka et al., 2014)

According to the manufacturer Leica Geosystems, using mobile systems, it is possible to achieve, on corresponding projects, a cost reduction of nearly 4 times compared to traditional methods, with an assumed accuracy of 1 cm. Additionally, the time spent in the field is reduced by a factor of 5.8, resulting in an overall 2.6 times faster completion of the entire project (GEFOS Leica, 2021).

2. RIEGL VMX-2HA

For the experiment, which will be further discussed, was used an MMS from the Austrian manufacturer Riegl, owned by the surveying office Nedoma & Řezník. For a simplified description of the system, it can be divided into three main components in terms of the vehicle: the internal part, located within the vehicle's interior; the external part, primarily positioned on the vehicle's roof; and the processing part, utilized for data collection and subsequent data processing.

2.1 Internal part MMS

This part of the system primarily responsible for data collection controlled from the operator's position, storing acquired data, and power-supplying the entire system.

Its main component is the Control Unit (CU), located in the luggage compartment. Essentially, it is a rugged computer equipped with a powerful 7th generation Intel Core i7 processor. Within the body of the suitcase, there are four slots for doubled 800GB SSD drives, providing ample storage capacity for capturing data of up to 6TB in size. Once the mission is completed, the SSD carriers can be removed from the CU, allowing for convenient transfer of the data for subsequent processing. The CU is operated by the operator through a touchscreen interface positioned in front of the co-pilot's seat.

The entire system is powered by two car batteries - one directly from the vehicle's power supply, and the other being an external backup battery. Additionally, the unit is equipped with four fuses that can be replaced in case of any issues. It can be connected to the internet network via LAN or Wi-Fi. Video output can be facilitated through HDMI and Display Port connections.

2.2 External part MMS

The part of the system primarily designed for data acquisition. Its main component, the Measuring Head (MH), is positioned on the roof of the vehicle within a rugged mounting bracket from which it can be detached. Additionally, the mounting bracket also includes a spherical camera, which, in certain types of installations, allows for its folding when not in use.

Another essential component is the Distance Measuring Indicator (DMI), which utilizes wheel rotations to maintain trajectory, especially in case of poor GNSS conditions. In addition to the parts that will be further described, the MH also houses a Trigger and Time-Stamping Unit, which ensures the synchronization of all data by precisely timestamping their acquisition (Riegl LMS, 2021).

Data transmission between the MH and CU occurs through a combined 10GigE Main Cable, which includes not only power and other cables but also optical fibers for fast transfer of a large amount of data. The transfer speed reaches 10 gigabits per second. The DMI is connected separately to the CU.

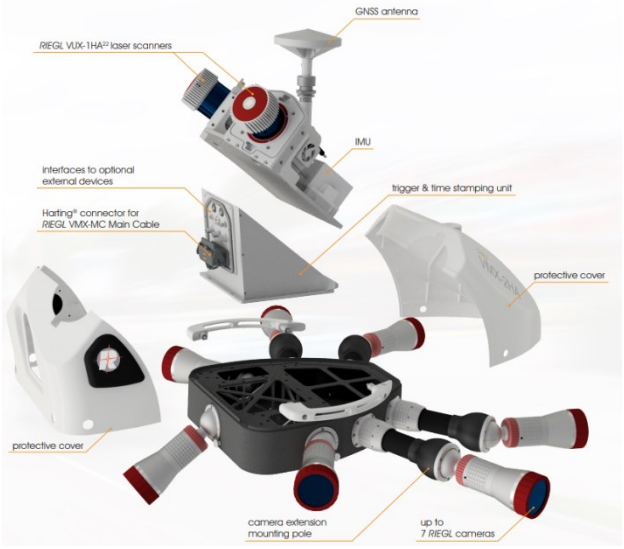

Figure 1. Components of Measuring Head. (Riegl LMS, 2021)

2.2.1 GNSS/IMU: The integration of the GNSS receiver with the AP540 antenna and the IMU unit POS LV 610 by Applanix provides a trajectory with an accuracy of 2-5 cm, along with odometry, for input into calculations. Prior to and after data collection, the entire system undergoes self-calibration using both the static and dynamic parts, which will be described in the paragraph dedicated to data collection. The GNSS/IMU system is operational within a temperature range of -20°C to +60°C. The IMU houses a Silicon accelerometer and a fiber optic gyroscope (FOG). (GEO-MATCHING, 2021)

The accuracies of GNSS/IMU in different directions during various outage times are provided in Table 1. During testing, the odometry was also included in the calculations. Based on these manufacturer-provided facts, there is a higher need for tie points in locations with poorer observational conditions.

GNSS/IMU						
outage [s]	0			60		
solution (RMS)	PP	IARTK	DGPS	PP	IARTK	DGPS
X,Y [m]	0,02	0,02	0,03	0,10	0,28	0,41
Z [m]	0,03	0,03	0,50	0,07	0,10	0,51
Roll & Pitch [deg]	0,0025	0,0050	0,0050	0,0025	0,0050	0,0050
True Heading [deg]	0,0150	0,0200	0,0200	0,0150	0,0200	0,0200

Table 1. Performance Specifications of used GNSS-IMU. (Applanix, 2021)

2.2.2 Scanners: The system is equipped with two VUX-1HA scanners that are positioned with a 70° horizontal offset from each other, and their horizontal axes form an angle of 39°. Thanks to their orientation, the amount of shadows in the resulting pointcloud is reduced. The scanner generation used in the surveying unit has a frequency of 1 MHz each and, by manufacturer, scans with an accuracy of 5 mm and precision of 3 mm (manufacturer-tested at a distance of 30 meters). It can capture up to 250 profiles (scans) per second, covering the entire field of view.

1,8 MHz program		distance					
		3 m		10 m		50 m	
platform speed	line spacing of a single scanner [mm]	point spacing within a scan/line of a single scanner [mm]	VMX-2HA point density [pts/m²]	point spacing within a scan/line of a single scanner [mm]	VMX-2HA point density [pts/m²]	point spacing within a scan/line of a single scanner [mm]	VMX-2HA point density [pts/m²]
50 km/h	56	2,6	13750	8,7	4100	44,0	820
80 km/h	89	2,6	8590	8,7	2570	44,0	510
120 km/h	133	2,6	5700	8,7	1700	44,0	340

Table 2. Point spacing. (Riegl LMS, 2021)

In the resulting pointcloud, a regullar pattern of scanning is visible, which is derived from the orientation of the scanners and can be observed in Figure 2. Each scanner generates rows of points that, due to the high rotation speed, can be considered parallel as they converge practically to infinity. The overlap of rows from both oriented scanners forms a checkerboard grid. The spacing between the lines can be adjusted apart from the settings by the vehicle's movement speed, while the distance between individual points within a line depends on the distance from the scanner and the set scanning frequency, independent of the vehicle's speed. (Grešla, 2022)

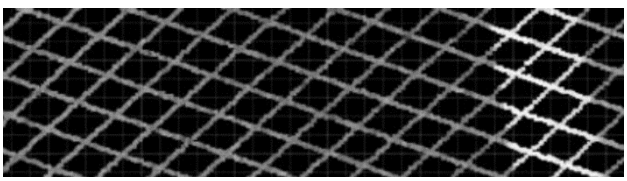

Figure 2. Scan pattern.

2.2.3 Cameras: Multiple cameras can be connected to the VMX-2HA system. As evident, seven of them can be directly connected to the sensor head. The rear three ports are on a movable joint, while the cameras attached to the front ports are connected via an extension rod with a joint. These cameras are primarily used for capturing detailed images of the area of interest. Prior to data collection, their field of view axis is adjusted using the mentioned joint. The manufacturer also offers a splitter reduction for the back port, which is for example recommended, when mapping cracks in the pavement to capture detailed images directly behind the vehicle.

In addition to cameras directly connected to the sensor unit, the manufacturer allows data collection from external cameras, which are typically spherical or thermal cameras. The recommended thermal camera by the manufacturer is the VarioCAM HD, which is capable of detecting rapid temperature changes. The pointcloud can be colored then based on temperature degrees.

Camera Options	max. numbers of cameras	max. frames* per second	resolution (H*V) [px]	lens focal length [mm]	Field of View [°]
5 MP CMOS	9	20	2464*2056	5	80,7*70,7
9 MP CMOS	9	10	4112*2176	8	83,1*50,3
12 MP CMOS	9	8	4112*3008	8	83,1*65,9
FLIR Ladybug 5+	1*6	19	6x 2048*2448	4,4	90% of full sphere
Nikon D810	9	1	8256*5504	14	104*81
				20	83*61

Table 3. Properties of supported cameras. (Riegl LMS, 2021)

*Maximum frame rate of a single camera operated in 8-bit mode. The use of multiple cameras may reduce maximum frame rates.

In general we can use equation:

$$V_{max} = d * f_{max} \quad (1)$$

where **V_{max}** = maximum vehicle speed in meter/second
d = trigger distance (between two consecutive images) in meter
f_{max} = maximum frame rate in fps (files/second)

The mentioned spherical camera is commonly used for colorization and other outputs. In our case, we are using the FLIR Ladybug5+ camera, which consists of six lenses and is positioned at the top of the sensor unit, as shown in Figure 3. The Ladybug camera is powered and triggered through a user interface located on the rear side of the sensor unit, but the captured images are stored in the control unit via USB 3.0. The saved files have the *.pgr extension and can be easily browsed using the Ladybug SDK software (Ladybug SDK, Ladybug Cap Pro, 2021), which allows viewing the captured images in various projections, editing them, and exporting them.

Figure 3. Mounting of cameras. (Riegl LMS, 2021)

2.3 Workstations

To process large-volume data, a powerful workstation with extensive SSD storage is required. The workstation used by GK Nedoma & Řezník is equipped with a dual AMD EYC processor (2x24 cores), 128 GB of RAM, and a total of 8TB SSD + 12TB HDD storage. In order to expedite the processing of multiple projects, a total of 3 similar PC workstations have been acquired. All workstations have frames for inserting carriers from the control unit (CU) to accelerate the transfer of captured data.

Based on experience, we can generally say that 1 km of scanned data, with the scanners set to their maximum frequency, an average data acquisition speed of 40 km/h, and capturing images from the Ladybug camera at 5m intervals, corresponds to approximately 4 GB of data.

3. ACQUISITION AND DATA PROCESSING

3.1 Control Points

To obtain the most accurate results, it is necessary to distribute an appropriate number of control points within the area of interest, which will be surveyed using conventional methods. The quantity of control points depends on the GNSS conditions in the given area, and it is logical that urban areas and forests require more control points compared to open terrain, where the GNSS conditions are optimal. The number of control points also depends on the desired output accuracy, which varies across different industries. The most commonly used type of control points for mobile mapping is a checkerboard with a standard size of 20 cm for the inner square. (Pavelka et al., 2012)

Figure 4. Signalisation of control points.

We need the precise coordinates of these control points for further calculations. Therefore, their surveying often takes place after the MMS acquisition, which requires favorable hydrometeorological conditions that cannot be predicted. Therefore, the crucial aspect is only the signalising of the control points within the area of interest before the MMS data collection.

3.2 Acquisition

After the system is connected and the vehicle is started, the system can be activated using the CU located in the cargo space.

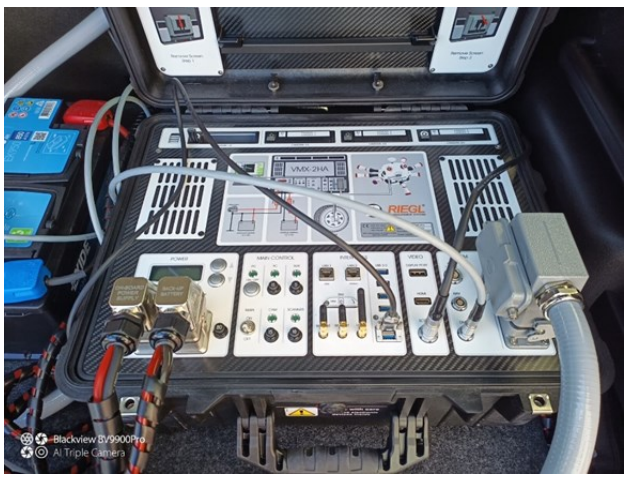

Figure 5. Mounted Control Unit.

Subsequently, a project is created on the control unit using the RiACQUIRE software (Riegl, RiACQUIRE, 2022) located at the co-driver's position. In this project, the operator adjusts various settings, including the scanning frequency and the distance or time interval for capturing images from the connected cameras. These settings can be different for each camera. Typically, a distance interval with a frequency of 5-10 m is chosen.

During the initialization and after the completion of data acquisition, it is necessary to perform a self-calibration of the INS/GNSS system. This calibration process consists of a 5-minute fast static method conducted in a location with excellent observation conditions, during which the vehicle must remain stationary without any movement. It is followed by a dynamic part where the vehicle moves in different directions, alternately decelerating and accelerating, and navigating through turns at appropriate speeds. The duration of the dynamic part depends on the observation conditions and typically lasts 10-15 minutes.

Upon entering the area of interest, the operator initiates the data recording and proceeds with multiple passes through the area of interest depending on the traffic density, which calls Multi Time Around (MTA). The vehicle's speed is selected based on the desired pointcloud density, and of course on speed limits. During the acquisition, the operator monitors the functionality of individual system components and guides the driver.

Figure 6. Operator's view during acquisition.

After the data acquisition is completed, the mentioned self-calibration is performed in the reverse order, and further work takes place in the office.

3.3 Processing

3.3.1 Trajectory and pointcloud: From the acquired INS/GNSS (+DMI) data and the generated virtual reference base station(s) in the area of interest, a post-processed trajectory is computed in the POSPac software (Applanix POSPac MMS, 2020). The trajectory is then imported into the manufacturer's processing software, RiPROCESS (Riegl, RiPROCESS, 2021), where the extraction of other acquired data takes place. In the next step, the acquired data is georeferenced to the post-processed trajectory. As mentioned before, all data is linked using Time-Stamp.

The next step to obtain a more accurate pointcloud is the adjustment using control points, for which we need coordinates in the specified coordinate system. During this adjustment, the MTA zones can also be apart of adjustment. This step significantly reduces the thickness of the pointcloud cross-section.

3.3.2 Camera data: During all steps, the trajectory is refined, which provides us with the precise position of the images. Their orientation is subsequently determined from identical points in the pointcloud. It is therefore necessary to find an image with an adequate number of appropriately distributed identical points for each camera, which is more challenging for a spherical camera.

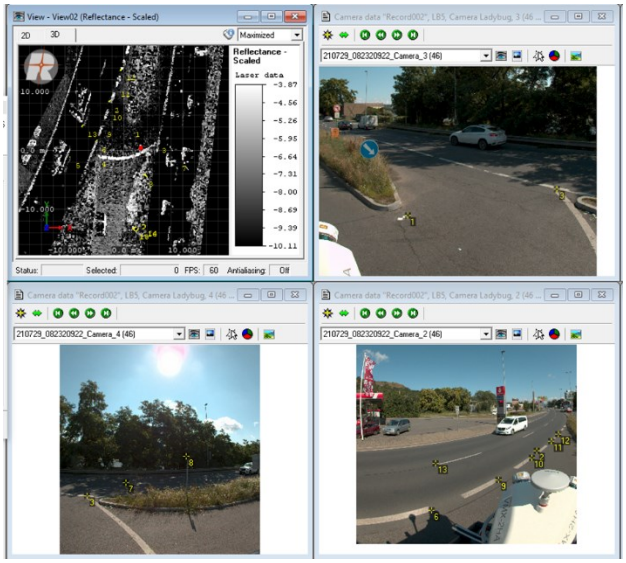

Figure 7. Example of spherical camera orientation. (RiPROCESS, 2021)

After camera orientation, the pointcloud can be colorized. Since every point is almost always present in more than one image, we can choose a statistical method to colorize the point.

Other steps offered by the manufacturer's software include, for example, the exclusion of isolated points, the exclusion of moving vehicles, or the classification of pointcloud.

4. EXPERIMENT

For testing the vertical accuracy of the MMS Riegl VMX-2HA, a 200m section of a new highway near Hradec Králové in the Czech Republic was selected, and control points were marked on it. The first acquisition took place several days after the final layer of Stone Mastic Asphalt (SMA) was laid. The area of interest was scanned twice by the mobile system, with an interval of nearly six months. During the period between the first and second scans, horizontal road markings were applied in the area, which prevented the use of the same control points for both missions.

During the individual computation steps, multiple pointclouds were exported. These pointclouds were later compared to demonstrate the improvement of results by each step.

As a control method was chosen usual terrestrial measurement with a total station connected to a local micro-network. In the given area, a total of 83 points were measured in a regular grid pattern, as shown in Figure 8. The pointcloud of these 83 points will be labeled as number 1.

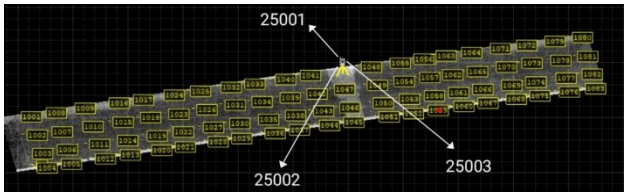

Figure 8. Scheme of terrestrial measuring.

From the first scan, which took place a few days after the placement of the SMA surface, we consider two pointclouds. The first one is aligned to the identical points measured from the highway control network (pointcloud 6), while the second one is subsequently aligned based on the MTA zones (pointcloud 5) for the entire scanned area, where our area of interest is only a subset. During the first scan, the surface was wet, resulting in the removal of a large number of points during the calculations.

The second scan was conducted 5 months after the first scan, and from this scan, we consider three pointclouds. The first one is without any alignments, only based on the Post-Process trajectory (pointcloud 2). The second one has the MTA zones mutually aligned (pointcloud 3), and the third one is subsequently aligned to the identical points measured from the local micro-network (pointcloud 4).

The comparison of the two pointclouds, with the denser one always serving as the reference, was performed in the CloudCompare software using the 2.5D triangulation method. This method selects the (k) nearest points from the reference pointcloud to the points being compared. From these points, it creates a Triangulated Irregular Network (TIN), and then calculates the vertical deviations (CloudCompare.org, 2019).

The following graph shows the comparison between pointcloud No. 1 (MS50) and pointcloud No. 4.

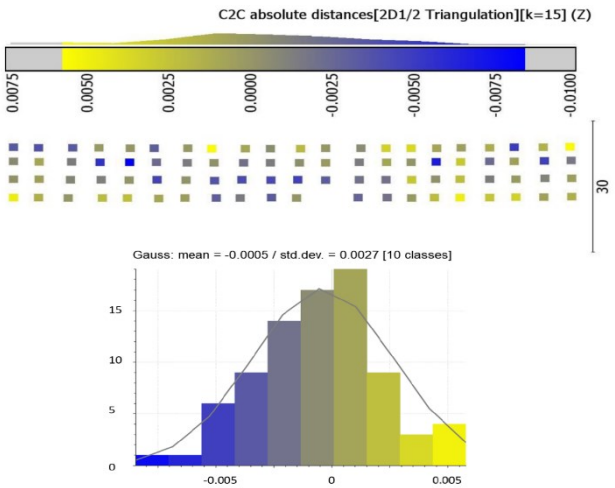

Figure 9. Residuals between pointcloud 1 and 4. (Grešla and Jašek, 2022)

The results of the other pointcloud comparisons using the same procedure can be seen in the following table, which demonstrates significant improvement achieved through individual computation steps. (Hampacher and Štroner, 2015)

Pointcloud 1 with: ↓	mean [m]	std.dev. [m]	**RMSe [m]**
2	0.0167	0.0098	**0.0194**
3	0.0047	0.0031	**0.0056**
4	-0.0005	0.0027	**0.0028**
6	0.0041	0.0059	**0.0072**
5	0.0023	0.0031	**0.0039**

Table 4. Results of cloud comparing.

The pointcloud 4 best approximates the results of the terrestrial measurement, while the pointcloud 2, which lacks all the alignments, deviates the most. In the comparison results between the terrestrial measurement and pointclouds 4 and 5, which are the most accurate pointclouds from two independent scans, we observe a difference of 1.1 mm, which could be attributed to

slight inhomogeneity in the GPS base station and micro-network or the extended area considered for alignment in pointcloud 5.

As part of the research, testing was conducted on different alignment procedures using the same initial pointcloud generated from data acquired during the second mission. From the results, we can conclude that it is more suitable to align first according to the MTA zones and then to the control points, although the difference does not show a significantly large value.

During the pointcloud testing, a comparison was also made between the first and second missions, which means comparing two pointclouds, always selecting the most accurate one for each mission. As can be seen in the following image, the comparison reveals the previously mentioned horizontal road markings, which appeared only in the second mission.

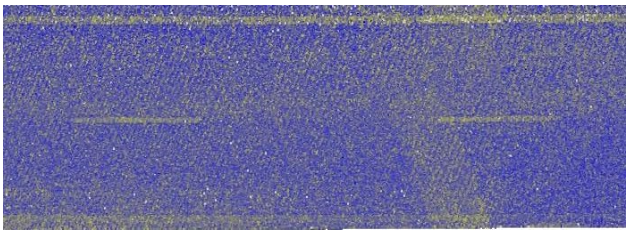

Figure 10. Results of comparing first and second mission.

5. CONCLUSIONS

Based on the obtained results, it can be concluded that data acquired by the mobile mapping unit, using the correctly chosen calculation procedure and a sufficiently dense network of control points with corresponding accuracy, can be utilized in a wide range of industrial sectors, including the inspection of road pavement layers.

An advantage of this method is that it provides a comprehensive understanding of the construction layer. From the obtained results, it is also evident that the second acquisition, which relies solely on INS/GNSS post-processing and is aligned using MTA, achieves very good results in terms of height accuracy. (Faltýnová and Pavelka, 2013)

REFERENCES

Applanix: APPLANIX POS LV DATASHEET [online]. [ref. 2023-05-10]. Available from: https://www.applanix.com/downloads/products/specs/POS-LV-Datasheet.pdf

Faltýnová, M.; Pavelka, K.: Mobile Laser Scanning for Highway Deformation Documentation, In: Proceedings of the 11th European Transport Congress. Praha: České vysoké učení technické v Praze, Fakulta dopravní, 2013. pp. 56-59. ISBN 978-80-01-05321-8.

GEFOS Leica: Leica PEGASUS:TWO Ultimate [online]. [ref. 2023-05-10]. Available from: https://www.gefos-leica.cz/data/original/skenery/mobilni-mapovani/two-ultimate/leica-pegasustwoultimate-ds-871011-0118-en-lr.pdf

GEO-MATCHING: APPLANIX POS LV 610 DATASHEET [online]. [ref. 2023-05-10]. Available from: https://geo-matching.com/inertial-navigation-systems-ins/pos-lv-610

GPS VAN [Coetsee, Josef, Brown, Alison, Bossler, John, "GIS Data Collection Using the GPSVan Supported by a GPS/Inertial Mapping System," Proceedings of the 7th International Technical Meeting of the Satellite Division of The Institute of Navigation (ION GPS 1994), Salt Lake City, UT, September 1994, pp. 85-93.

Grešla, O.: Bachelor Thesis - Comparison of the accuracy of the mobile mapping system with the terrestrial method and the acquisition of this device [ref. 2023-05-10], Praha: Czech Technical University in Prague, 2022. Available from https://dspace.cvut.cz/handle/10467/102940 (In Czech)

Hampacher, M. - Štroner, M.: Zpracování a analýza měření v inženýrské geodézii. 2. vyd. Praha: Česká technika - nakladatelství ČVUT, ČVUT v Praze, 2015. 336 s. ISBN 978-80-01-05843-5. (In Czech)

Jašek, P., Grešla, O., 2022 Experiences in measuring roads using a scanning vehicle. 14. mezinárodní konference Geodézie a kartografie v dopravě. 1. Praha: Český svaz geodetů a kartografů, z.s., 2022. s. 155-167. ISBN: 978-80-02-02990-8. (In Czech)

Pavelka, K.; Faltýnová, M.: Joining of MMS and ALS Data with Orthophoto; a Case Project: Highway Deformation Detection and Visualization, In: Proceedings of ACRS 2012. Chang Wattana Road, Bangkok: Asian Association of Remote Sensing (AARS), 2012. pp. 2335-2343. Geo-Informatics and Space Technology Development Agency. ISBN 978-1-62276-974-2.

Pavelka, K.; Faltýnová, M.; Švec, Z.; Dušánek, P.: Mobilní laserové skenování, Praha: Czech Technical University in Prague, 2014. ISBN 978-80-01-05261-7. (In Czech)

Riegl VMX-2HA: BROCHURE [online]. [ref. 2023-05-10]. Available from: http://www.riegl.com/uploads/tx_pxpriegldownloads/RIEGL_VMX-2HA_brochure_2022-10-27.pdf